LES OF INHOMOGENEOUS CANOPY FLOWS USING TERRESTRIAL LASER SCANNING DATA

Fabian Schlegel and Jörg Stiller
Technische Universität Dresden
Institute of Fluid Mechanics
01062 Dresden, Germany
{fabian.schlegel, joerg.stiller}@tu-dresden.de

ABSTRACT

The effect of sub-tree forest heterogeneity in the flow past a clearing is investigated by means of large-eddy simulation (LES). For this purpose, a detailed representation of the canopy has been acquired by terrestrial laser scanning (TLS). The scanning data is used to produce a high resolution plant area distribution (PAD). For the LES study, the PAD is embedded in a larger domain covered with an idealised, horizontally homogeneous canopy. Simulations are performed for neutral conditions and compared to an LES with homogeneous PAD. The study reveals a considerable influence of small-scale plant distribution on the mean velocity field as well as on turbulence data. Particularly near the edges of the clearing, where canopy structure is highly variable, usage of a realistic PAD appears to be crucial for capturing the local flow structure. Inside the forest, local variations in plant density induce a complex pattern of up and downward motions, which remain visible in the mean flow.

INTRODUCTION

Understanding the interaction between plant canopies and the atmospheric boundary layer is of considerable interest for a broad range of applications including meteorology, agriculture, forestry and biology. For a general overview about this topic we refer to the surveys of Raupach & Thom (1981); Finnigan (2000); Langre (2008).

Under certain conditions, e.g., within uniform stands, the canopy can be considered horizontally homogeneous and isotropic. Further common simplifications involve the negligence of structural diversity, flexibility and elasticity of plant parts. With these assumptions it is possible to characterise the canopy by a so-called plant area density depending on the vertical direction only. In addition, a drag coefficient is introduced for relating the PAD to the flow resistance caused by the vegetation. The flow above and within such (quasi) homogeneous canopies has been investigated extensively in various field studies, laboratory experiments and numerical simulations that helped to gain insight into the fundamental transport mechanisms, e.g., Finnigan *et al.* (2009); Watanabe (2009).

As the flow over a forest edge can be viewed as a generic model for the first type of heterogeneity, various studies put a focus on it (e.g. Raynor (1971); Gash (1986); Irvine *et al.* (1997); Lee (2000); Belcher *et al.* (2003); Yang *et al.* (2006*b*,*a*); Cassiani *et al.* (2008); Dupont & Brunet (2008, 2009); Dupont *et al.* (2011)). In most of these investigations vegetation was assumed to be horizontally homogeneous.

Bohrer *et al.* (2009) presented the first and so far only numerical study considering the aerodynamic effect of vertical and horizontal heterogeneities down to scales matching the crown size. The canopy data were produced with the virtual canopy generator V-CaGe, developed by Bohrer *et al.* (2007). The simulations indicated that heterogeneity decreases the displacement height and increases the roughness length and penetration depth to be used in regional models. On the smaller scale, the heterogeneity pattern influences the spatial distribution of ejection and sweep events. As a result, so-called ejection and sweep hot spots develop, which can affect local gas exchange and particle transport significantly.

The numerical simulation of such a heterogeneous canopy requires a highly resolved, digital image of the vegetation. Within this area, photogrammetry has seen a rapid development over the last few years and is now regularly applied in forest inventory (see, e.g. Aschoff & Spiecker (2004); Maas *et al.* (2008); Vosselman & Maas (2010)). Complemented by appropriate postprocessing methods these techniques produce 3D distributions of the plant area density and further attributes, which reproduce forest morphology in a realistic way. Our objective is to take a first step in combining the promising opportunities of laser scanning with the potential of large-eddy simulation and to explore the viability of this approach as a tool for investigating the flow over heterogeneous forest stands at sub-tree resolution.

DESCRIPTION OF THE FIELD SITE

Subject of investigation is a clearing located in the forest “Tharandter Wald” about 25km southwest of the city of Dresden in Germany ($50^\circ 57' 49''$ N, $13^\circ 34' 01''$ E and 380 m a.s.l.). The site accommodates an anchor station operated by the Institute of Hydrology and Meteorology of TU Dresden since 1958, which has been used in various European projects, e.g. EuroFlux (Bernhofer *et al.* (2003)) and CarboEurope IP (Gruenwald & Bernhofer (2007)).

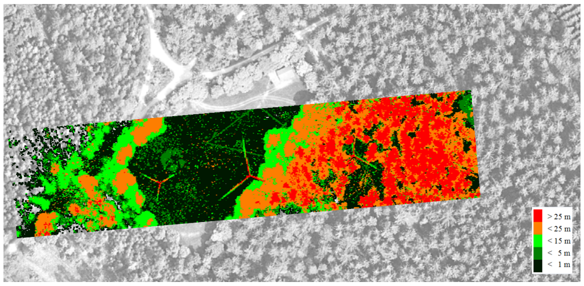

Figure 1. Aerial view of the field site with the investigation area marked and colored by vegetation height, Bienert *et al.* (2010).

The site consists of a forest stand seeded in 1887 and a clearing of about $50\,\mathrm{m} \times 90\,\mathrm{m}$, named "Wildacker". The stand is characterised by a dense canopy with a mean height of about $h = 35\,\mathrm{m}$ and an open trunk space with sparse understory. A detailed description and stand parameters could be found in Feigenwinter *et al.* (2004). The investigated domain, marked by the frame in Fig. 1, is aligned according to the predominant wind direction of West to East and includes the clearing. In summer 2008, one permanent and three temporarily built up measurement towers were used during a measurement campain. The permanent scaffolding tower stands 100 m west of the clearing inside a nearly homogeneous forest area and has a height of 42 m. This tower is used as reference position for this study.

TERRESTRIAL LASER SCANNING

Laser scanning is an efficient 3D measurement technique which is being used in an increasing range of application fields, including the acquisition of forest inventory parameters, see e.g., Vosselman & Maas (2010). The scanning procedure is described in Bienert *et al.* (2010) and Fig. 2 shows the virtual forest as seen by the laser scanner. After a geometric registration of all performed scans (13 ground positions for this study) the unorganised point cloud is converted into a voxel representation. This is accomplished using a ray tracing method, which allows for identifying voxels that are penetrated by laser pulses before hitting an object. The minimum voxel size is limited by the density and precision of the data points. State-of-the-art terrestrial laser scanners allows a voxel size of less than 10 cm, which is far beyond the needs of the present study. Therefore, with respect to the minimum mesh size used in the numerical simulations, a voxel size of 1 m was chosen. The plant area density, which is required in the numerical model, results from the reflection property by the application of plant specific clumping factor, see Ryu *et al.* (2010).

NUMERICAL METHOD

For the presented study neutral atmospheric conditions are assumed and the domain size is less than one kilometer. Therefore, variations in density and the influence of Coriolis force can be neglected. Hence, the flow is governed by the incompressible Navier-Stokes equations. Within the LES approach, the resolved and the unresolved or subgrid scales are separated from each other by using a filter operation. Application of the filter to the Navier-Stokes equations yields the resolved-scale or LES equations in the form

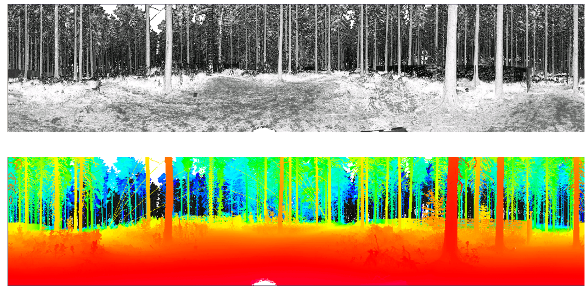

Figure 2. 2D-amplitude image (top) and range image (bottom) of a laser scan

$$\partial_t \overline{u}_i + \partial_j \left(\overline{u}_j \overline{u}_i\right) = -\partial_i \overline{p} + \partial_j \left(2\nu \overline{S}_{ij}\right) + \partial_j \tau_{ij} + \overline{f}_{i,d} + \overline{f}_{i,p} \tag{1}$$

$$\partial_i \overline{u}_i = 0 \tag{2}$$

where $\overline{\mathbf{u}}$, $\overline{p}$ are the resolved velocity and pressure, $\overline{S}_{ij} = \left(\partial_i \overline{u}_j + \partial_j \overline{u}_i\right)/2$ the strain rate tensor and

$$\tau_{ij} = -\left(\overline{u_i u_j} - \overline{u}_i \overline{u}_j\right) \tag{3}$$

the so-called SGS stresses, which have to be modelled. Following the approach of Shaw & Schumann (1992) the plant drag results from the local wind speed $|\overline{\mathbf{u}}|$ and the plant area density a augmented by an empirical drag coefficient c_d,

$$\overline{f}_{i,d} = -c_d a \left|\overline{\mathbf{u}}\right| \overline{u}_i \tag{4}$$

The last term in Eqn. (1) represents the effect of the mesoscale pressure gradient that is imposed to maintain a prescribed bulk velocity under the presence of periodic boundary conditions.

To approximate the SGS stresses (3) we use the one-equation model of Deardorff (1980) with the extensions for canopy flows introduced by Shaw & Schumann (1992). In frame of this model the stresses are related to the resolved strain rate tensor by

$$\tau_{ij} = 2\nu_r \overline{S}_{ij} - \frac{2}{3}\delta_{ij}\overline{k''} \tag{5}$$

where

$$\nu_r = C_\nu \ell \overline{k''}^{1/2} \tag{6}$$

is the SGS viscosity and $\overline{k''} = \overline{u_i'' u_i''}/2$ the unresolved turbulent kinetic energy (TKE). The model is closed by the SGS energy transport equation

$$\partial_t \overline{k''} + \partial_j \left(\overline{u}_j \overline{k''}\right) = \tau_{ij}\overline{S}_{ij} + \partial_j \left(2\nu_r \partial_j \overline{k''}\right) - C_E \frac{\overline{k''}^{3/2}}{\ell} - \frac{2\overline{k''}}{\tau} \tag{7}$$

where the last two terms model dissipation and the bypass effect associated with the enhanced breakdown of large structures in the canopy with time scale $\tau = \overline{u}_i / \overline{f}_{i,d}$.

The LES equations (1,7) are discretised using a cell-centred finite volume method (Ferziger & Peric (1996)) and implemented using the OpenFOAM® CFD toolbox 1.6. The method employs the TVD fluxes of Sweby (1984) for convective terms and central differences for diffusive fluxes and SGS stresses. A backward differencing scheme of second order accuracy in conjunction with the PISO algorithm for enforcing continuity (Issa (1985)) serves for time integration. In order to reduce the computational cost, the scheme involves an iterative procedure for evaluating the convective terms, Jasak (1996). For details of the numerical method and implementation we refer to Weller *et al.* (1998).

RESULTS

The intention of the present study is to investigate the feasibility of using laser scanning data for LES of canopy flows and to gain some insight into the effect of smallscale plant heterogeneity. In principle it would be possible to consider the fully threedimensional PAD determined at the field site. However, since the TLS postprocessing was constricted to a strip of 30 m width and 191 m length (including the clearing), we decided to use a simplified PAD, which represents the lateral average over the strip. The computational domain is chosen as a compromise between the desired resolution and the dimensions that are necessary to accommodate the dominant coherent structures (Finnigan *et al.* (2009); Dupont & Brunet (2009)) and to allow for flow adjustment behind the clearing (Yang *et al.* (2006*a*,*b*)). It extends over $760\,\mathrm{m} \times 210\,\mathrm{m} \times 380\,\mathrm{m}$ in the streamwise, lateral and vertical directions, respectively. The first test case incorporates the clearing as a plant-free section that starts at $x = -60\,\mathrm{m}$ and extends to $x = 0\,\mathrm{m}$. The forest stand is characterised by a homogeneous PAD determined by a forrest assessment of six harvested Norway spruces. The second case is defined by replacing the idealised PAD by the lateral average of the measured PAD in a section including a part of the lee-side edge, the whole clearing and approximately 120 m of the adjacent, windward forest stand.

All computations were performed using periodic boundary conditions in the streamwise and lateral directions, no slip conditions at the bottom and free slip at the top. For discretisation we used a non-equidistant grid consisting of $220 \times 190 \times 82$ cells with a spacing of 2 m in a subdomain stretching from $x = -1.5h$ to $6.5h$ and $z \leq 4h$. Outside this region the streamwise and the vertical spacing were gradually increased to 6 m.

Mean Velocity

To get an idea of the flow structure near the clearing, the the streamwise and vertical velocity components are plotted in Fig. 3. In both cases the streamlines reveal a weak recirculation zone, which extends almost over the whole clearing (zero contour line in Fig. 3(a) and 3(c)). The presence of a recirculation zone in front the windward forest edge leads to a flow pattern that differs qualitatively from the picture obtained for isolated edges or long clearings, e.g. Yang *et al.* (2006*a*); Dupont & Brunet (2009). Instead of being expulsed, the flow penetrates the canopy from above in a short section adjacent to the edge. A significant influence of the plant distribution is evident from the contour plots of the streamwise and vertical velocity components. While the streamwise velocity contours evolve a similar pattern as for the homogeneous stand for $x/h > 1.2$, the vertical component (Fig. 3(b) and 3(d)) varies considerably within and above the heterogeneous patch. Except of the region very close to the edge these variations are closely linked with the smallscale heterogeneity of the PAD. Since the extremal values of the mean vertical velocity reach up to three percent of the reference velocity, one may expect that local changes in plant density give rise to a significant transport of mass and momentum through the canopy that cannot be captured with the assumption of a homogeneous PAD.

Turbulence Statistics

Fig. 4 depicts the distributions of the mean turbulent energy and the Reynolds stress. In both cases, the turbulent fluctuations intensify in the shear layer separating the recirculation zone and the outer flow passing the clearing. For the homogeneous canopy we observe an intrusion of TKE into the trunk space, as reported previously, e.g., by Dupont *et al.* (2011). In contrast turbulence decays quickly while passing the denser and largely closed edge in case with heterogeneous PAD (Fig. 4(d)). Generally, however, the effect of small-scale plant distribution is less visible than for the vertical velocity. The Reynolds stress decays faster within the edge in heterogeneous case due to the denser PAD. It is worth noting, however, that the Reynolds stress attains its maximum before turbulent kinetic energy.

ACKNOWLEDGEMENT

The work was supported by the German National Science Foundation (Deutsche Forschungsgemeinschaft, DFG) within the DFG priority programme 1276 MetStröm: Multiple Scales in Fluid Mechanics and Meteorology. Computational facilities were provided by the Centre for Information Services and High Performance Computing (ZIH) of the TU Dresden.

REFERENCES

Aschoff, T. & Spiecker, H. 2004 Algorithms for the automatic detection of trees in laser scanner data. *International Archives of Photogrammetry, Remote Sensing and Spatial Information Sciences* **XXXVI - 8/W2**, 71 – 75.

Belcher, S.., Jerram, N. & Hunt, J. 2003 Adjustment of a turbulent boundary layer to a canopy of roughness elements. *Journal of Fluid Mechanics* **488**, 369 – 398.

Bernhofer, C., Aubinet, M., Clement, R., Grelle, A., Gruenwald, T., Ibrom, A., Jarvis, P., Rebmann, C., Schulze, E. & Tenhunen, J. 2003 *Fluxes of Carbon, Water and Energy of European Forests*, *Ecological Studies*, vol. 163, chap. Spruce forests (Norway and Sitka spruce, including Douglas fir): Carbon and water fluxes and balances, ecological and ecophysiological determinants, pp. 99 – 123. Springer.

Bienert, A., Queck, R., Schmidt, A., Bernhofer, C. & Maas, H.-G. 2010 Voxel space analysis of terrestrial laser scans in forests for wind field modelling. *International Archives of Photogrammetry, Remote Sensing and Spatial Information Sciences* **XXXVIII - Part 5**, 92 – 97.

Bohrer, G., Katul, G., Walko, R. & Avissar, R. 2009 Exploring the effects of microscale structural heterogeneity of forest canopies using large-eddy simulations. *Boundary-Layer Meteorology* **132**, 351 – 382.

Bohrer, G., Wolosin, M., Brady, R. & Avissar, R. 2007 A virtual canopy generator (v-cage) for modelling complex heterogeneous forest canopies at high resolution. *Tellus B* **59**, 566 – 576.

Cassiani, M., Katul, G. & Albertson, J. 2008 The effects of canopy leaf area index on airflow across forest edges: large-eddy simulation and analytical results. *Boundary-Layer Meteorology* **126**, 433 – 460.

Deardorff, J. 1980 Stratocumulus-capped mixed layers derived from a three-dimensional model. *Boundary-Layer Meteorology* **18**, 495 – 527.

Dupont, S., Bonnefond, J.-M., Irvine, M., Lamaud, E. & Brunet, Y. 2011 Long-distance edge effects in a pine forest with a deep and sparse trunk space: in situ and numerical experiments. *Agricultural and Forest Meteorology* **151**, 328 – 344.

Dupont, S. & Brunet, Y. 2008 Edge flow and canopy structure: a large-eddy simulation study. *Boundary-Layer Meteorology* **126**, 51 – 71.

Dupont, S. & Brunet, Y. 2009 Coherent structures in canopy edge flow: a large-eddy simulation study. *Journal of Fluid Mechanics* **630**, 93 – 128.

Feigenwinter, C., Bernhofer, C. & Vogt, R. 2004 The influence of advection on the short term co2 - budget in and above a forest canopy. *Boundary-Layer Meteorology* **113**, 201 – 224.

Ferziger, J. & Peric, M. 1996 *Computational Methods for Fluid Dynamics*. Springer-Verlag Berlin Heidelberg.

Finnigan, J. 2000 Turbulence in plant canopies. *Annual Review of Fluid Mechanics* **32**, 519 – 571.

Finnigan, J., Shaw, R. & Patton, E. 2009 Turbulence structure above a vegetation canopy. *Journal of Fluid Mechanics* **637**, 387 – 424.

Gash, J. 1986 Observations of turbulence downwind of a forest-heath interface. *Boundary-Layer Meteorology* **36**, 227 – 237.

Gruenwald, T. & Bernhofer, C. 2007 A decade of carbon, water and energy flux measurements of an old spruce forest at the anchor station tharandt. *Tellus Series B* **59**, 387 – 396.

Irvine, M., Gardiner, B. & Hill, M. 1997 The evolution of turbulence across a forest edge. *Boundary-Layer Meteorology* **84**, 467 – 496.

Issa, I. 1985 Solution of the implicitly discretised fluid flow equations by operator-splitting. *Journal of Computational Physics* **62**, 40 – 65.

Jasak, H. 1996 Error analysis and estimation for the finite volume method with applications to fluid flows. PhD thesis, Imperial College of Science, London.

Langre, E. 2008 Effects of wind on plants. *Annual Review of Fluid Mechanics* **40**, 141 – 168.

Lee, X. 2000 Air motion within and above forest vegetation in non-ideal conditions. *Forest Ecology and Management* **135**, 3 – 18.

Maas, H.-G., Bienert, A., Scheller, S. & Keane, E. 2008 Automatic forest inventory parameter determination from terrestrial laserscanner data. *International Journal of Remote Sensing* **29** (5), 1579 – 1593.

Raupach, M. & Thom, A. 1981 Turbulence in and above plant canopies. *Annual Review of Fluid Mechanics* **13**, 97 – 129.

Raynor, G. 1971 Wind and temperature structure in a coniferous forest and a contiguous field. *Forest Science* **17**, 351 – 363.

Ryu, Y., Nilson, T., Kobayashi, H., Sonnentag, O., Law, B. & Baldocchi, D. 2010 On the correct estimation of effective leaf area index: Does it reveal information on clumping effects? *Agricultural and Forest Meteorology* **150**, 463 – 472.

Shaw, R. & Schumann, U. 1992 Large-eddy simulation of turbulent flow above and within a forest. *Boundary-Layer Meteorology* **61**, 47 – 64.

Sweby, P. 1984 High resolution schemes using flux limiters for hyperbolic conservation laws. *SIAM Journal on Numerical Analysis* **21** (5), 995 – 1011.

Vosselman, G. & Maas, H.-G. 2010 *Airborne and Terrestrial Laser Scanning*. Whittles Publishing.

Watanabe, T. 2009 Les study on the structure of coherent eddies inducing predominant perturbations in velocities in the roughness sublayer over plant canopies. *Journal of the Meteorological Society of Japan* **87** (1), 39 – 56.

Weller, G., Tabor, G., Jasak, H. & Fureby, C. 1998 A tensorial approach to computational continuum mechanics using object-oriented techniques. *Computers in Physics* **12** (6), 620 – 631.

Yang, B., Raupach, M., Shaw, R., U, K. Paw & Morse, A. 2006*a* Large-eddy simulation of turbulent flow across a forest edge. part i: flow statistics. *Boundary-Layer Meteorology* **120**, 377 – 412.

Yang, B., Shaw, R. & U, K. 2006*b* Wind loading on trees across a forest edge: a large eddy simulation. *Agricultural and Forest Meteorology* **141**, 133 – 146.

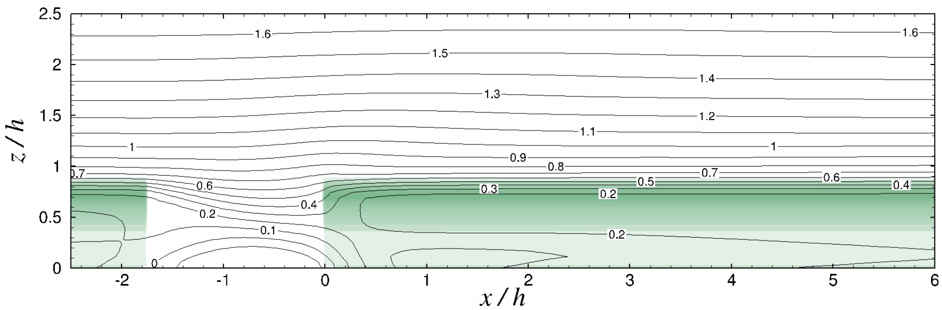

(a) Streamwise velocity for simulation with homogeneous plant area density

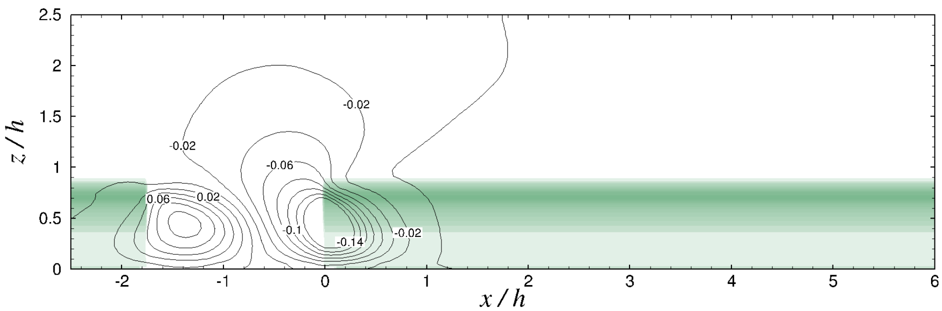

(b) Vertical velocity for simulation with homogeneous plant area density

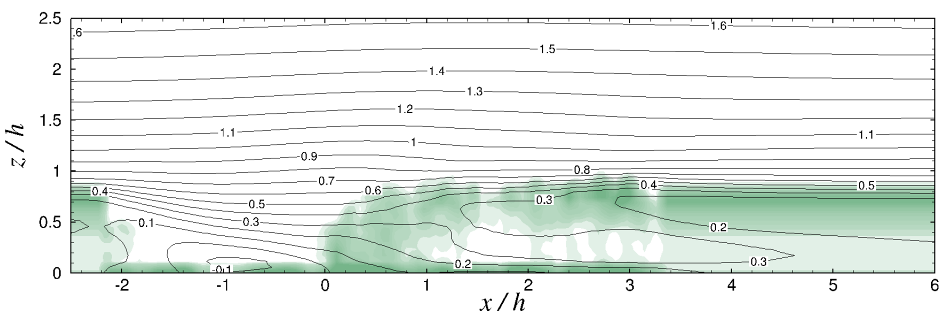

(c) Streamwise velocity for simulation with heterogeneous plant area density

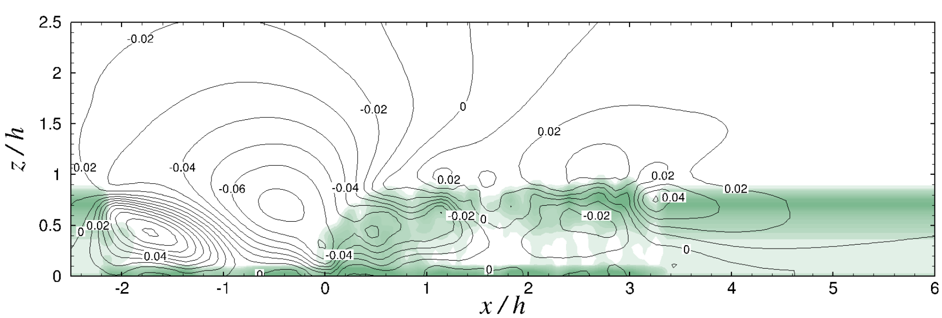

(d) Vertical velocity with heterogeneous plant area density

Figure 3. Mean velocity distribution for simulations with homogeneous (a,b) and heterogeneous (c,d) plant area density. The mean velocity is normalized with the velocity at permanent scaffolding tower located at $x/h = 3h$ in 42 m height. The colouring depicts the plant area density. The mean canopy height h is about 35 m.

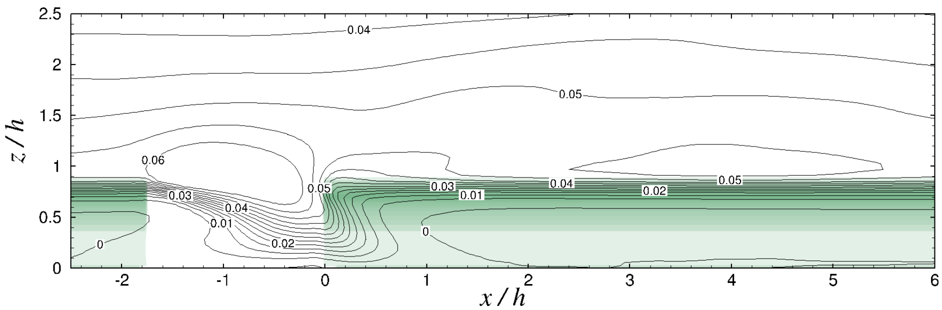

(a) Reynolds stress for simulation with homogeneous plant area density

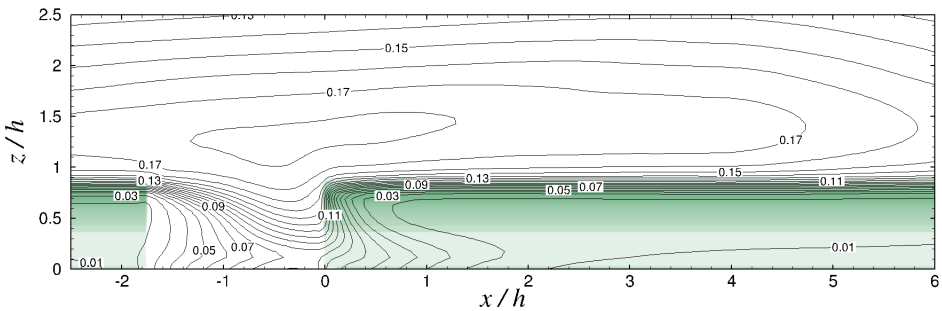

(b) Turbulent kinetic energy for simulation with homogeneous plant area density

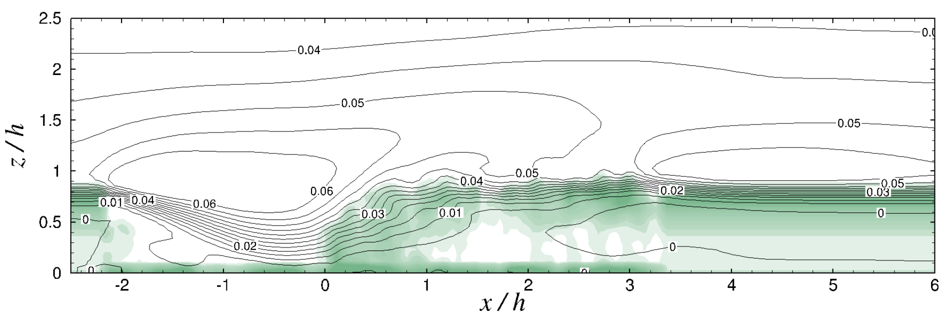

(c) Reynolds stress for simulation with heterogeneous plant area density

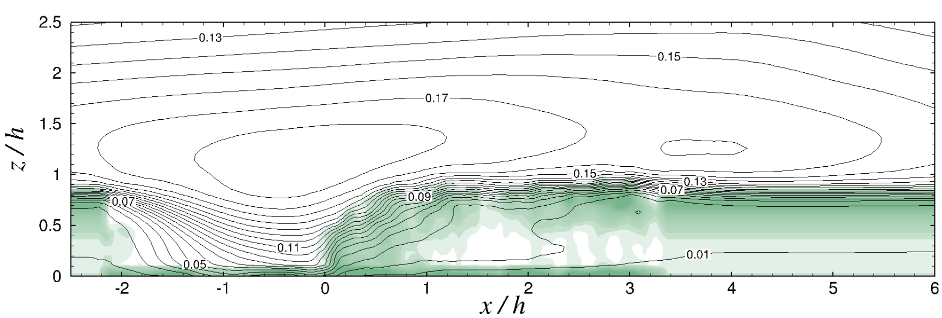

(d) Turbulent kinetic energy with heterogeneous plant area density

Figure 4. Turbulent energy and Reynolds stress for simulations with homogeneous (a,b) and heterogeneous (c,d) plant area density. Both values are normalized with the square of velocity at permanent scaffolding tower located at $x/h = 3h$ in 42 m height. The colouring depicts the plant area density. The mean canopy height h is about 35 m.